Talanta 134 (2015) 298–304

Contents lists available at ScienceDirect

Talanta

journal homepage: www.elsevier.com/locate/talanta

G-quadruplex DNA/protoporphyrin IX-based synergistic platform for targeted photodynamic cancer therapy

Zhixue Zhou, Dan Li, Libing Zhang, Erkang Wang*, Shaojun Dong*

State Key Laboratory of Electroanalytical Chemistry, Changchun Institute of Applied Chemistry, Chinese Academy of Sciences, Changchun, Jilin 130022, People's Republic of China Graduate School of the Chinese Academy of Sciences, Beijing 100039, People's Republic of China

ARTICLE INFO

Article history:
Received 19 August 2014
Received in revised form
14 November 2014
Accepted 19 November 2014
Available online 28 November 2014

Keywords:
G-quadruplex
Nuclease
Protoporphyrin IX
Photodynamic therapy
Cancer

ABSTRACT

Photodynamic therapy (PDT) is an emerging technique to induce cancer cell death. However, the tumor specificity, cellular uptake and biodistribution of many photosensitizers urgently need to be improved. In this regard, we show here that the integrated nanoassemblies based on G-quadruplex DNAs (GQDs)/protoporphyrin IX (PPIX) can serve as a synergistic platform for targeted high-performance PDT. In the nanoassemblies, GQDs function as carriers of sensitiser PPIX and confers the system cancer cell targeting ability. After nucleolin-mediated efficient binding and cellular uptake of GQDs/PPIX assemblies, the strong red fluorescence of GQDs/PPIX complex provides a powerful tool for biological imaging. Moreover, the reactive oxygen species (ROS) generated by GQDs/PPIX under light illumination can effectively kill cancer cells. The present approach is simply composed by DNA and photosensitizers, thereby avoiding any complicated and time-consuming covalent modification or chemical labeling procedure.

1. Introduction

It is more than 25 years since photodynamic therapy (PDT) was proposed as a useful tool in oncology [8,14]. Since then, thousands of patients have been treated. Although PDT has progressed surely in the past decades, its use remains marginal. There exist some unfavorable features that need to be solved. For example, protoporphyrin IX (PPIX) is a well-known photodynamic agent in cancer therapy [5,25]. However, the following disadvantages limit its usefulness in PDT: (1) the poor water solubility of PPIX limits its direct application for PDT [5,9,28]; (2) PPIX is a poor tumor or cancer cell localizer [26]. Since the cytotoxic product, $^1O_2$, can migrate less than 0.02 μm after its formation [29], the localization of PPIX is important for valid cancer therapy and minimizing damage to healthy tissues; (3) for efficient PDT, sensitizers are expected to be taken by cells. If PDT sensitizers do not accumulate in cell nuclei, PDT has generally a low potential of causing DNA damage, mutations, and carcinogenesis [30]; (4) PPIX is biosynthesized in low amounts by all tumor cells [27]. Very recently, platinum–porphyrin conjugates have been used in the construction of PDT system with improved cellular uptake and biodistribution of porphyrins [31]. Although promising, such system requires sophisticated synthesis processes, which adds to the complexity, cost, and overall assay time. Therefore, it would be highly desirable to develop PDT system that is simple in design, feasible to accumulate in cancer cells, and involves a reliable, efficient treatment.

Toward this goal, herein, we develop an integrated nanoplatform based on G-quadruplex DNAs (GQDs)/PPIX assemblies for targeted high-performance PDT. The primary motivations for employing GQDs lie in the fact that they can capture PPIX with high affinity and remarkably promote the fluorescence of PPIX [21], also they themselves exhibit active therapeutic effect as aptamers or non-antisense antiproliferative agents [3,11]. Of particular interest, some GQDs can bind to a specific cellular protein (GQD-binding protein, which has been tentatively identified as nucleolin) and become internalized. Inspired by these unique features, we propose a new approach for efficient PPIX-based PDT:GQDs act as PPIX carriers and hold PPIX dispersed. Meanwhile, GQDs loaded with PPIX target cancer cells and achieve binding and internalization by cells. Sequentially treatment with irradiation, the ROS generated by GQDs/PPIX complex under light illumination can effectively kill cancer cells. Yet, as oligonucleotides-related treatments, the excellent resistance of DNA probes to degradation by nucleases is vital for potential biomedical applications [3,22,23]. Although the stability problem of DNA probes has been largely addressed by using oligonucleotides with chemical modifications, these approaches may not be appropriate in the case of GQDs. Even tiny modifications in quadruplex aptamers may significantly alter their three-dimensional structure and preclude binding to their intended target [12]. Therefore, we first investigate the anti-nuclease cleavage abilities of unmodified GQDs, and select GQDs with excellent nuclease resistance for further PDT experiments. Intriguingly, one GQD, named T30695, is found to well resist nuclease

* Corresponding authors. Tel.: +86 431 85262101; fax: +86 431 85689711.
E-mail address: dongsj@ciac.ac.cn (S. Dong).

http://dx.doi.org/10.1016/j.talanta.2014.11.039
0039-9140/

cleavage whatever the cationic nature of the buffer. Such uniqueness of T30695 ensures the present PDT system reliability and usefulness. Thus, the integration of T30695 and PPIX makes it a potentially new tool for targeted cancer imaging and high-performance PDT. Compared with many nanoparticles-based PDT approaches [10,4], the present strategy is only constructed by DNA and photosensitiser, and might avoid any complicated and time-consuming covalent modification or chemical labeling procedure.

2. Materials and methods

2.1. Chemicals and materials

Oligonucleotides with specific sequences (which are listed in Table S1) were synthesized by Shanghai Sangon Biotechnology Co. Ltd. (Shanghai, China). The concentrations of oligonucleotides were determined using the 260 nm UV absorbance with the corresponding extinction coefficient. Deoxyribonuclease I (DNase I) (7×10^4 U/mL) was purchased from TaKaRa Biotechnology Co. Ltd (Dalian, China). Protoporphyrin IX (PPIX) and tris (hydroxymethyl) aminomethane (Tris) were obtained from Alfa Aster. All other chemicals were of analytical grade and used without further treatment. All stock and buffer solutions were prepared using ultrapure water ($>$ 18 MΩ) from a Milli-Q Plus system (Millipore). The pH values were determined by SARTORIUS PB-10 Standard pH meter.

2.2. Nuclease resistance

The solutions of GQDs (0.4 μM) in Na^+ (0.2 M) or K^+ (0.2 M) solution were heated at 90 °C for 5 min and slowly cooled down to room temperature. Then DNase I was added and incubated for 0.5 h. As for fluorescence spectroscopic analysis, PPIX (0.4 μM) in T-Buffer (10 mM Tris–HNO_3, pH 7.0, 100 mM KNO_3) was mixed with the prepared solutions and allowed to react for another 0.5 h. The fluorescence of the mixture was then measured at room temperature.

2.3. Fluorescence spectroscopic analysis

The fluorescence emission spectra were collected from 570 to 750 nm using a Fluoromax-4 spectrofluorometer (HORIBA Jobin Yvon, Inc., NJ, USA) at room temperature. The excitation wavelength was set at 410 nm.

2.4. Circular dichroism (CD) measurements

The CD spectra of DNAs (5 μM) were collected by a JASCO J-820 spectropolarimeter (Tokyo, Japan), of which the lamp was always kept under a stable stream of dry purified nitrogen (99.99%) during experiments. Three scans from 220 to 350 at 0.1 nm intervals were accumulated and averaged. The background of the buffer solution was subtracted from the CD data. For the thermal melting experiments, the samples were covered with mineral oil to avoid evaporation. The temperature was taken from 10 to 90 °C. The rate of temperature rise was set as 1 °C/min, and balance time was set as 1 min. The thermal melting experiments in the presence of Na^+ were performed at 260 nm, 297 nm, and 297 nm for T30695, PW17, PS2.M, respectively. The thermal melting experiments in K^+ solution were performed at 260 nm for the three GQDs. The antiparallel quadruplexes have a CD spectrum characterized by a positive ellipticity maximum at 295 nm and a negative minimum at 265 nm, while the parallel type have a positive maximum at 264 nm and a negative minimum at 240 nm.

2.5. Native polyacrylamide gel electrophoresis (PAGE)

The DNA solutions mixed with 6 × loading buffer were analyzed in 15% native polyacrylamide gel. The electrophoresis was conducted in 1 × TBE (pH 8.2) at constant voltage of 130 V for 1.5 h. The gels were first immersed in 25% isopropanol for 15 min, and then stained in the Stains-All solution at dark for 4 h, followed by destaining in water under moderate light. Finally, the gels were photographed with a personal camera.

2.6. Confocal laser scanning microscopy (CLSM)

HeLa and HEK 293 cells were incubated with T30695/PPIX or PPIX in the incubator for 2 h, and then washed with PBS for three times before investigated by CLSM (TCS SP2, Leica, Germany). The fluorescence micrographs shown are representative of at least three independent experiments.

2.7. Cell viability assay

Methyl thiazolyl tetrazolium (MTT) assay was used to evaluate the cytotoxicity of T30695, PPIX and T30695/PPIX. When cells reached 80% confluency, they were harvested and seeded in 96-well plates (10^4 cells per well) and cultured in the cell incubator for 24 h. The cells were incubated with various concentrations of above substances in dark conditions for 24 h. Then 10 μL MTT solution (5 mg/mL) was added to each well and the cells was cultured in the incubator for another 4 h. The medium was removed and 100 μL DMSO was added to completely lyse the cells. The absorbance at the wavelength of 570 nm for the cell lysate was measured using Tecan Infinite M200 (Switzerland). Cell viability was calculated by the following equation: cell viability $= [A_{570}]_{test}/[A_{570}]_{control} \times 100$, where $[A]_{test}$ was the absorbance of the test cells treated with therapeutics, and $[A]_{control}$ was the absorbance of cells without treatment. The experiments were performed independently for at least three times.

2.8. Irradiation-induced cytotoxicity

Cells were grown as indicated above in 96-well plates to reach 10^4 cells per well. Cells were incubated with T30695/PPIX nanoassemblies for 2 h, and then cells were washed several times with PBS. After that, 100 μL fresh cell culture medium was added into each well. For photodynamic therapy (PDT), the plates were illuminated for 10 min by 450 nm light (5 mW/cm^2). Finally, cells were incubated in a humidified atmosphere with 5% CO_2 at 37 °C for another 24 h. Then, standard MTT assay was carried out to determine the cell viabilities relative to the control untreated cells.

3. Results and discussion

3.1. Design of GQDs/PPIX-based high-performance PDT

The approach for GQDs/PPIX-based PDT is shown in Fig. 1A: (1) GQDs bind PPIX with high affinities, and GQDs binding holds PPIX dispersed, thereby avoiding its aggregation into low-fluorescence micelles; (2) GQDs/PPIX targets nucleolin, which is over-expressed in cancer cells compared to normal cells; (3) nucleolin could shuttle between the nucleus and cytoplasm, thus mediating the binding and uptake of GQDs/PPIX in cancer cells; (4) the strong red fluorescence from GQDs/PPIX complex shows promising application in targeted cancer cell imaging and early-stage cancer diagnosis; (5) upon irradiation with light, an efficient and cancer cells-specific PDT can be achieved. Previous studies of the therapeutic potential of GQDs mainly focus on two aspects: one is that some GQDs can inhibit proliferation and induce apoptosis in cancer cell lines [3,11]; another is

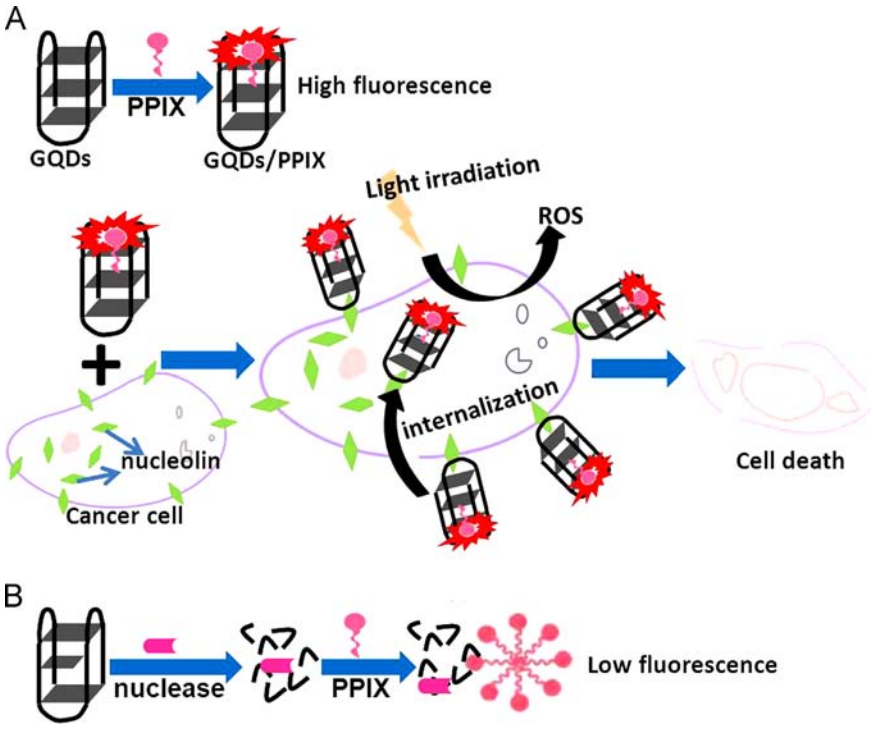

Fig. 1. (A) Schematic illustration of the irradiation activated GQDs/PPIX system for cancer cell-specific PDT. (B) Schematic illustration of the analysis of nuclease resistance of GQDs.

that GQDs are involved in the activity regulation of telomerase [40,32,2,38], and compounds which can stabilize human telomeric G-quadruplex can be potential anticancer agent [36,20,6,37]. Herein, we expect that the present work could offer a unique opportunity to GQDs for application in PDT.

3.2. Optimization of GQDs with enhanced nuclease-resistance

Given that the nuclease resistance of DNA-based medicines is critical when used in living cells, we therefore hope to choose GQDs with excellent nuclease resistance so as to achieve reliable and efficient cancer treatment. DNase I [1,19], a common endonuclease, was employed to assess the nuclease stability of GQDs [22,23].

GQDs can form a variety of possible quadruplex structures, depending on the base sequence and buffer conditions (especially the presence of monovalent cations such as K^+ and Na^+). For example, quadruplexes can be formed by one, two or four molecules of single-stranded DNA (ssDNA), which are referred to as monomer, dimer and tetramer structures, respectively. To simplify the system, we mainly focus on the monomer quadruplexes for the subsequent studies. Three model GQDs, whose structural characteristics have been determined previously by nuclear magnetic resonance (NMR) and/or X-ray crystallographic (XRC) techniques, are first investigated. They are named as T30695 [13], PW17 [33] and PS2.M [24], respectively. Native polyacrylamide gel electrophoresis (PAGE) and fluorescence spectroscopy are utilized to study the nuclease resistance of GQDs in K^+ or Na^+ solutions. The basic principles are as follows: (1) If GQDs are hydrolyzed by nucleases, then weakened bands of GQDs in PAGE would be observed; (2) these GQDs can remarkably promote the fluorescence of PPIX (Fig. 1A). If GQDs are degraded by nucleases, PPIX would return to the state of aggregation, accompanied by a sharp decrease in fluorescent intensity (Fig. 1B).

Fig. 2 depicts the utilization of CD spectra and thermal denaturation experiments to identify the formed quadruplex structures. In Na^+ solution, T30695 mostly folds into parallel quadruplex structure (curve a, Fig. 2A). In contrast, the CD spectrum of PS2.M

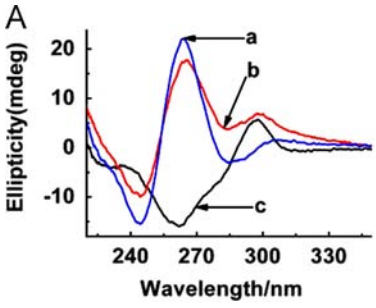

Na^+-stabilized	T30695	PW17	PS2.M
T_m(℃)	70	59	54

Fig. 2. (A) CD spectra of different GQDs in the presence of Na^+: (a) T30695; (b) PW17; (c) PS2.M. (B) CD-melting curves for (1) PS2.M, (2) PW17, (3) T30695 in Na^+ solution. The calculated T_m values for Na^+-stabilized quadruplexes are listed in the following table. The pH value for the experiments was 7.0.

shows characteristics of antiparallel G-quadruplexes (curve c, Fig. 2A). As for PW17, the CD spectrum suggests the formation of parallel/antiparallel mixed structures (curve b, Fig. 2A). Furthermore, the thermal stabilities (T_m) of the three GQDs were calculated based on the thermal denaturation experiments (Fig. 2B), and the

calculated T_m values suggest that the three GQDs fold into stable Na^+-stabilized G-quadruplexes at room temperature. Moreover, the spectra in Fig. 3 reveal that these GQDs can remarkably promote the fluorescence of PPIX (curves 1→2, Fig. 3A–C). However, after reaction with DNase I, only T30695 system still promote the fluorescence of PPIX (curve 3, Fig. 3A), while PW17 and PS2.M systems seriously lose these functions. These observations suggest that, in the presence of Na^+, only T30695 demonstrates excellent anti-nuclease cleavage ability. Next, the PAGE experiments were further used to test the cleavage of GQDs. The 16-mer ssDNA and dsDNA are chosen as internal migration standards. As shown in Fig. 3D, the band representing T30695 (lane 3, Fig. 3D) shows no evident change after T30695 is treated with DNase I (lane 4, Fig. 3D). However, in the case of PS2.M and PW17, weakened bands are observed after their treatment with DNase I (lanes 5→6 and 7→8, Fig. 3D). The obtained results further confirm that T30695 indeed demonstrates excellent nuclease resistance ability.

In the case of K^+-stabilized G-quadruplexes, the three GQDs all fold into parallel quadruplex structures (Fig. 4A). Thermal denaturation experiments (Fig. 4B) show that the three GQDs are stabilized preferentially by K^+, accompanied by high T_m values. As for the nuclease resistance, according to the fluorescent results in Fig. 5A–C, after reaction with DNase I, the three GQDs can still promote the fluorescence of PPIX, indicating that quadruplex structures formed in the presence of K^+ are more nuclease-resistant than those formed in the presence of Na^+. The results of native PAGE experiments in Fig. 5D also validate these results. The bands representing T30695 (lane 3, Fig. 5D), PS2.M (lane 5, Fig. 5D) and PW17 (lane 7, Fig. 5D) show no evident change after they are treated with DNase I (lane 4, lane 6 and lane 8 in Fig. 5D, respectively). However, it is noteworthy that even in the presence of 200 mM K^+, still apparent fluorescence decrease can be observed for PS2.M/PPIX and PW17/PPIX systems after reaction with DNase I (Fig. 5B and C), which is absolutely unsuitable for practical applications.

Taken together, it is clear that T30695 can well resist nuclease cleavage whatever the cationic nature of the buffer. Previous research has demonstrated that guanine nucleotides within the core of a G-quadruplex are relatively protected from chemical attack, and the loops in GQDs give the chance for nuclease cleavage [3,39,34]. Thus, it is possible that the three single-nucleotide loops in T30695 (Fig. S1) are not easily attacked by nucleases, resulting in the super anti-cleavage ability of T30695. To probe further the role of loops in nuclease resistance of GQDs, the other two GQDs, named G_3T_4TT and $G_3T_4TT_4$, are designed through extending the single-nucleotide loops in T30695 [35]. In the presence of Na^+ or K^+, G_3T_4TT, with one four-base thymine loop (T4 loop), maintains parallel quadruplex structures (Fig. S2); while $G_3T_4TT_4$ with two T4 loops adopts antiparallel structures (Fig. S3). The fluorescent results, presented in Figs. S4 and S5, clearly reveal that the nuclease resistance of G_3T_4TT and $G_3T_4TT_4$ with long loops is apparently poorer than T30695.

It appears that not all GQDs exhibit nuclease resistance afforded by the quadruplex structure, and in some cases, even with the aid of large amount of K^+, the G-quadruplex structures still can be destroyed by nuclease. These findings might facilitate the correction of previous thought that GQDs have favorable biostability [3]. In addition, this work, combined with previous demonstrations, indicates that the loops of quadruplexes play important role in the degradation of GQDs, and GQDs with long loops are more easily attacked by nuclease. Given that the aim of the present study is to identify GQDs with high resistance to nuclease, we thus choose T30695 as viable probe for next application in PDT.

3.3. T30695/PPIX-based synergistic nanoplatform for targeted PDT

We probe further the usefulness of T30695/PPIX nanoassemblies in PDT system. Fig. 6A shows the photographs of T30695/PPIX nanoassemblies and PPIX under irradiation with excitation source.

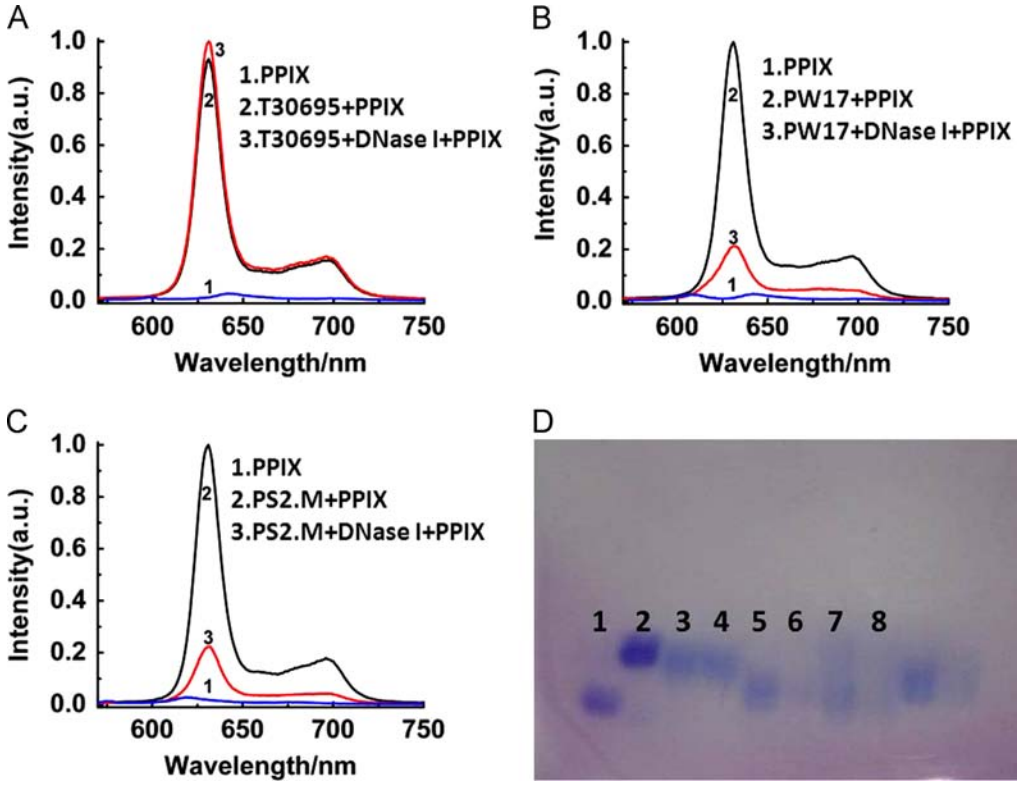

Fig. 3. Fluorescent analysis (A–C) of GQDs degraded by DNase I in the presence of Na^+. (D) Native PAGE analysis of Na^+-stabilized GQDs degraded by DNase I. Lane1: a 16-mer ssDNA; Lane 2: a 16-mer dsDNA; Lane 3: T30695; Lane 4: T30695+DNase I; Lane 5: PS2.M; Lane 6: PS2.M+DNase I; Lane 7: PW17; Lane 8: PW17+DNase I. The 16-mer ssDNA and dsDNA are chosen as internal migration standards.

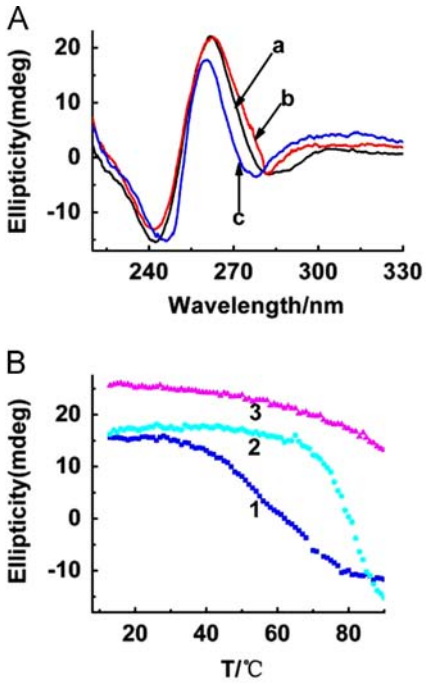

K⁺-stabilized	T30695	PW17	PS2.M
T_m(℃)	>75	>75	66

Fig. 4. (A) CD spectra of different GQDs in the presence of K^+: (a) T30695; (b) PW17; (c) PS2.M. (B) CD-melting curves for (1) PS2.M, (2) PW17, (3) T30695. The calculated T_m values for K^+-stabilized quadruplexes are listed in the following table.

Compared with PPIX, the nanoassemblies exhibit strong red fluorescence, ascribed to the enhancement of the fluorescence of PPIX. More importantly, the red fluorescence of T30695/PPIX system is unaffected in the presence of DNase I under physiological conditions. Next, to confirm the target ability of T30695/PPIX, HeLa cells (nucleolin overexpressed) and HEK 293 cells (normal cells) are chosen as target cancer cells and control cells, respectively. Cells were incubated with T30695/PPIX for 2 h. It is evident from the fluorescence imaging experiments (Fig. 6B) that the bright red fluorescent T30695/PPIX covers the cell membrane or enters into HeLa cells. As for HEK 293 cells, no distinct fluorescence was observed (Fig. S6). These results imply the specific interaction between T30695 and nucleolin overexpressed on HeLa cells and the internalization of T30695/PPIX mediated by nucleolin. In addition, competition experiments, using free PPIX, were also performed. As shown in Fig. S7, no significant fluorescence is observed in HeLa cells, which also indicates that nucleolin is responsible for the efficient binding and cellular uptake of T30695/PPIX. Thus, the conjugation of T30695 to PPIX successfully renders the system cancer cell-targeting ability.

Having demonstrated the specific internalization experiments, we then proceed to realize PDT mediated cell killing. The standard MTT assay was carried out to evaluate the cytotoxicity of T30695, PPIX and T30695/PPIX complex towards HeLa cells with various concentrations. As shown in Fig. 6C, the results reveal that neither T30695 nor PPIX demonstrates toxicity towards HeLa cells even at high concentrations up to 20 μM, whereas T30695/PPIX complex exhibits certain cytotoxic effect against HeLa cells, most notably at 4 μM. Previous research has pointed out that seven days after the addition of T30695, the proliferation of HeLa cervical carcinoma cells can be inhibited [11]. In the present work, it is possible that due to the

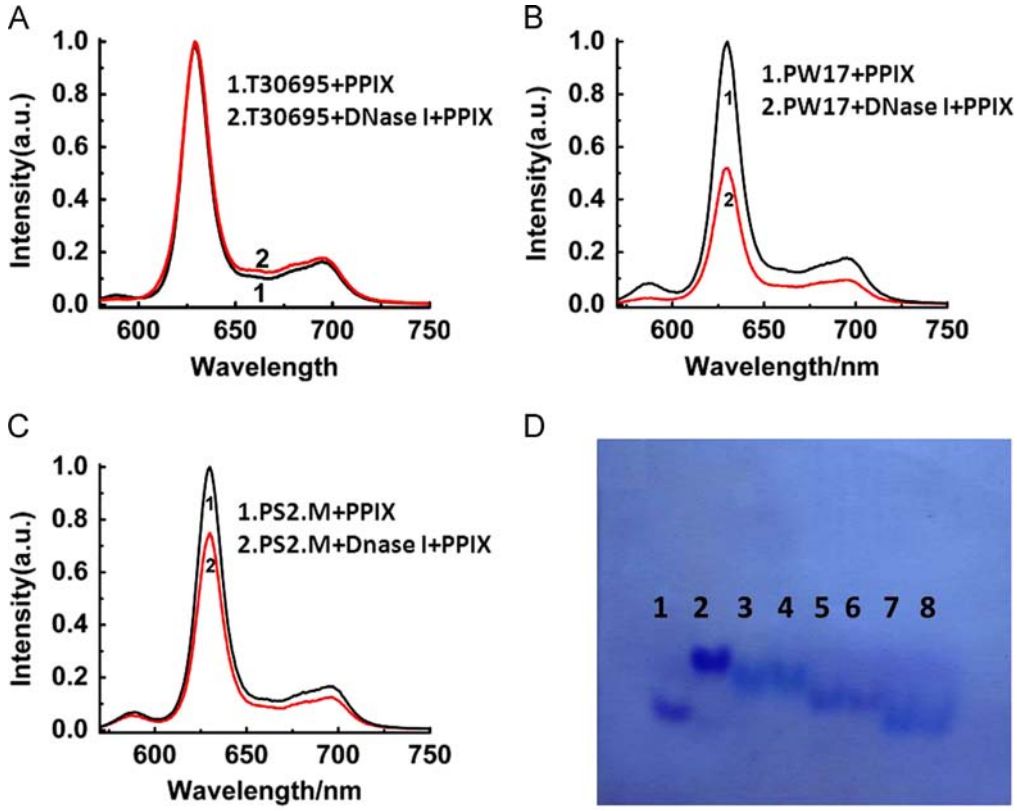

Fig. 5. (A–C) Fluorescent analysis of K^+-stabilized GQDs degraded by DNase I. (D) Native PAGE analysis of GQDs degraded by DNase I in the presence of K^+. Lane1: a 16-mer ssDNA; Lane 2: a 16-mer dsDNA; Lane 3: T30695; Lane 4: T30695+DNase I; Lane 5: PS2.M; Lane 6: PS2.M+DNase I; Lane 7: PW17; Lane 8: PW17+DNase I. The 16-mer ssDNA and dsDNA are chosen as internal migration standards.

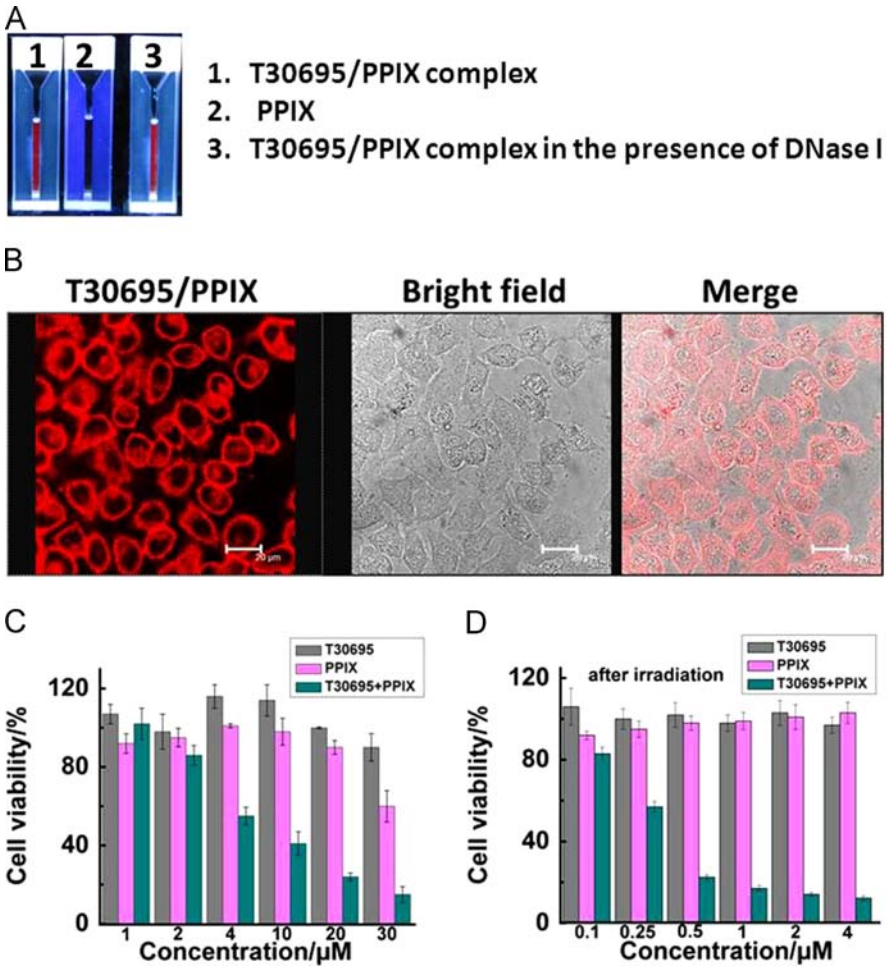

Fig. 6. (A) Photographs of various solutions obtained under irradiation with excitation source: (1) T30695/PPIX complex; (2) PPIX; (3) T30695/PPIX complex in the presence of DNase I. (B) Fluorescence images of HeLa cells incubated with T30695/PPIX for 2 h. Scale bars are 20 μm. (C) Cell viability of HeLa cells after administration with equal concentrations of T30695, PPIX and T30695/PPIX for 24 h. (D) Cell viability of HeLa cells incubated with T30695, PPIX and T30695/PPIX after light irradiation. Error bars represent strand deviation of three independent experiments.

short incubation time, T30695 exhibit faint antiproliferative effects. Under light illumination, as low as 0.25 μM T30695/PPIX complex resulted in a significant cytotoxicity (Fig. 6D). In control experiments, even 4 μM PPIX induce negligible cytotoxicity towards cancer cells after light irradiation (Fig. 6D). Undoubtedly, T30695/PPIX complex shows significantly higher efficacy in inhibition of tumor cell growth compared to PPIX alone, mainly because the targeting property of T30695 allows a higher amount of T30695/PPIX to bind the cell surface and to be internalized by the HeLa cells. Accordingly, compared to the anti-proliferative effects of T30695 with long incubation time, modulation of cellular ROS absolutely improves treatment efficiency. These results evidently substantiate the synergistic platform for efficient targeted cancer therapy.

4. Conclusions

In summary, we have demonstrated that the integrated GQDs/PPIX nanocomposite could serve as a synergistic platform for targeted high-performance PDT. This approach is simple in design, and can largely address the problems of tumor specificity, cellular uptake and biodistribution of PPIX in PDT process. Although much research interest has been directed to improving the tumor specificity of photosensitizers by conjugating them with tumor-associated antibodies [16,7], there are problems associated with the use of monoclonal antibodies in PDT. These include complicated synthesis, transport barriers and poor biostability ([14,17,18,15]). Compared with these earlier approaches, the present DNA aptamer-based strategy demonstrates increased biostability, efficient cellular uptake, and avoids extensive modifications. Combined together, it is expected that our work can be a step forward in development of PDT as a routine treatment for cancer.

Acknowledgement

This work was supported by the Natural Science Foundation of China (no. 21375123), and 973 projects (no. 2011CB911002).

Zhixue Zhou and Dan Li contributed equally to this work.

Appendix A. Supporting information

Supplementary data associated with this article can be found in the online version at http://dx.doi.org/10.1016/j.talanta.2014.11.039.

References

[1] S. Anderson, Nucleic Acids Res. 9 (13) (1981) 3015–3027.
[2] S. Balasubramanian, L.H. Hurley, S. Neidle, Nat. Rev. Drug Discovery 10 (4) (2011) 261–275.

[3] P.J. Bates, D.A. Laber, D.M. Miller, S.D. Thomas, J.O. Trent, Exp. Mol. Pathol. 86 (3) (2009) 151–164.
[4] D. Bechet, P. Couleaud, C. Frochot, M. Viriot, F. Guillemin, Trends Biotechnol. 26 (11) (2009) 151–164.
[5] J. Bedwell, A.J. MacRobert, D. Phillips, S.G. Bown, Br. J. Cancer 65 (6) (1992) 818–824.
[6] M. Bejugam, S. Sewitz, P.S. Shirude, R. Rodriguez, R. Shahid, S. Balasubramanian, J. Am. Chem. Soc. 129 (43) (2007) 12926–12927.
[7] M. Birchler, F. Viti, L. Zardi, B. Spiess, D. Neri, Nat. Biotechnol. 17 (10) (1999) 984–988.
[8] S.B. Brown, E.A. Brown, I. Walker, Lancet Oncol. 5 (8) (2004) 497–508.
[9] S.B. Brown, M. Shillcock, P. Jones, Biochem. J. 153 (2) (1976) 279–285.
[10] Z. Chen, Z. Li, J. Wang, E. Ju, L. Zhou, J. Ren, X. Qu, Adv. Mater. 24 (4) (2013) 522–529.
[11] V. Dapic, V. Abdomerovic, R. Marrington, J. Peberdy, A. Rodger, J.O. Trent, P.J. Bates, Nucleic Acids Res. 31 (8) (2003) 2097–2107.
[12] V. Dapić, P.J. Bates, J.O. Trent, A. Rodger, S.D. Thomas, D.M. Miller, Biochemistry 41 (11) (2002) 3676–3685.
[13] N.Q. Do, K.W. Lim, M.H. Teo, B. Heddi, A.T. Phan, Nucleic Acids Res. 39 (21) (2011) 9448–9457.
[14] D.E.J.G.J. Dolmans, D. Fukumura, R.K. Jain, Nat. Rev. Cancer 3 (5) (2003) 380–387.
[15] S.W. Friedrich, S.C. Lin, B.R. Stoll, L.T. Baxter, L.L. Munn, R.K. Jain, Neoplasia 4 (5) (2002) 449–463.
[16] M.R. Hamblin, J.L. Miller, T. Hasan, Cancer Res. 56 (22) (1996) 5205–5210.
[17] R.K. Jain, Adv. Drug Deliv. Rev. 46 (1-3) (2001) 149–168.
[18] R.K. Jain, Nat. Med. 4 (6) (1998) 655–657.
[19] N. Kienzle, D. Young, S. Zehntner, G. Bushell, T.B. Sculley, Biotechnique 20 (4) (1996) 612.
[20] M.-Y. Kim, H. Vankayalapati, K. Shin-ya, K. Wierzba, L.H. Hurley, J. Am. Chem. Soc. 124 (10) (2002) 2098–2099.
[21] T. Li, E. Wang, S. Dong, Anal. Chem. 82 (18) (2010) 7576–7580.
[22] N. Li, C. Chang, W. Pan, B. Tang, Angew. Chem. Int. Ed. 51 (30) (2012) 7426–7430.
[23] N. Li, Z. Yu, W. Pan, Y. Han, T. Zhang, B. Tang, Adv. Funct. Mater. 23 (18) (2013) 2255–2262.
[24] P.R. Majhi, R.H. Shafer, Biopolymers 82 (2006) 558–569.
[25] Z. Malik, H. Lugaci, Br. J. Cancer 56 (5) (1987) 589–595.
[26] Z. Malik, M. Djaldetti, Int. J. Cancer 26 (4) (1980) 495–500.
[27] Z. Malik, M. Djaldetti, Cell Differ 8 (3) (1979) 223–233.
[28] T.B. Melo, G. Reisaeter, Biophys. Chem. 25 (1) (1986) 99–104.
[29] J. Moan, K. Berg, Photochem. Photobiol. 53 (4) (1991) 549–553.
[30] J. Moan, Photochem. Photobiol. 43 (6) (1986) 681–688.
[31] A. Naik, R. Rubbiani, G. Gasser, B. Spingler, Angew. Chem. Int. Ed. 53 (27) (2014) 6938–6941.
[32] R.J. O 'Sullivan, J. Karlseder, Nat. Rev. Mol. Cell Biol. 11 (3) (2010) 171–181.
[33] V. Pavlov, Y. Xiao, R. Gill, A. Dishon, M. Kotler, I. Willner, Anal. Chem. 76 (7) (2004) 2152–2156.
[34] Y. Peng, X. Li, J. Ren, X. Qu, Chem. Commun. 48 (2007) 5176–5178.
[35] P.A. Rachwal, I.S. Findlow, J.M. Werner, T. Brown, K.R. Fox, Nucleic Acids Res. 35 (12) (2007) 4214–4222.
[36] M. Read, R.J. Harrison, B. Romagnoli, F.A. Tanious, S.H. Gowan, A.P. Reszka, W.D. Wilson, L.R. Kelland, S. Neidle, Proc. Natl. Acad. Sci. U.S.A. 98 (9) (2001) 4844–4849.
[37] J.E. Reed, A.A. Arnal, S. Neidle, R. Vilar, J. Am. Chem. Soc. 128 (18) (2006) 5992–5993.
[38] J.F. Riou, L. Guittat, P. Mailliet, A. Laoui, E. Renou, O. Petitgenet, F. Megnin-Chanet, C. Helene, J.L. Mergny, Proc. Natl. Acad. Sci. U.S.A. 99 (5) (2002) 2672–2677.
[39] D. Sun, L.H. Hurley, J. Med. Chem. 52 (9) (2009) 2863–2874.
[40] Y. Xu, Chem. Soc. Rev. 40 (5) (2011) 2719–2740.